Physica D ▮ (▮▮▮▮) ▮▮▮–▮▮▮

Contents lists available at ScienceDirect

Physica D

journal homepage: www.elsevier.com/locate/physd

Metrics for ergodicity and design of ergodic dynamics for multi-agent systems

George Mathew [a,*], Igor Mezić [b]

[a] Embedded Systems and Networks Group, United Technologies Research Center (UTRC), Inc., Berkeley, CA, USA
[b] Department of Mechanical Engineering, University of California, Santa Barbara, CA, USA

ARTICLE INFO

Article history:
Received 10 December 2009
Received in revised form
26 October 2010
Accepted 27 October 2010
Available online xxxx
Communicated by V. Rom-Kedar

Keywords:
Ergodicity
Uniform sampling
Multi-agent systems
Control

ABSTRACT

In this paper we propose a metric that quantifies how far trajectories are from being ergodic with respect to a given probability measure. This metric is based on comparing the fraction of time spent by the trajectories in spherical sets to the measure of the spherical sets. This metric is shown to be equivalent to a metric obtained as a distance between a certain delta-like distribution on the trajectories and the desired probability distribution. Using this metric, we formulate centralized feedback control laws for multi-agent systems so that agents trajectories sample a given probability distribution as uniformly as possible. The feedback controls we derive are essentially model predictive controls in the limit as the receding horizon goes to zero and the agents move with constant speed or constant forcing (in the case of second-order dynamics). We numerically analyze the closed-loop dynamics of the multi-agents systems in various scenarios. The algorithm presented in this paper for the design of ergodic dynamics will be referred to as Spectral Multiscale Coverage (SMC).

© 2010 Elsevier B.V. All rights reserved.

1. Introduction

Ergodic theory studies the time-averaged behaviour of dynamical systems. A system is said to exhibit *ergodic dynamics* if it visits every subset of the phase space with a probability equal to the *measure* of that subset. Birkhoff's ergodic theorem states that a dynamical system is ergodic if and only if the time averages of functions along trajectories are equal to their spatial averages (see [1]). Much of the research in ergodic theory deals with analyzing the ergodicity (or lack of) for specific dynamical systems. There are relatively few studies that deal with the problem of designing ergodic dynamics. This is the subject of this paper. First, we propose metrics to quantify how far trajectories are from being ergodic. Then, we use this metric for the design of ergodic dynamics for multi-agent systems. An interesting application of this work is cooperative control of mobile robotic/sensor networks to achieve uniform coverage of a domain.

Cooperative control of mobile robotic/sensor networks is an emerging discipline with a lot of recent research activity. This is partly due to the various advances in robotic technologies and networks and partly due to the interesting mathematical challenges that arise from cooperative control problems. A recent example for an interesting advance in robotic technology is the MIT Robofish [2] that mimics the movement of real fish with few components. In the near future, one can envision a school of such robofish performing cooperative tasks in the ocean like surveillance and environmental monitoring. For working prototypes of mobile sensor networks see [3,4].

The emergence of cooperative control as a discipline can be affirmed by special journal issues dedicated entirely to various problems in cooperative control. See [5,6] for special issues presenting papers that deal with a wide range of coordination tasks such as consensus, connectivity maintenance, formation stabilization, coverage and target detection. See [7] for a special issue dedicated to coordinated control of many, mobile, networked sensor platforms for ocean state estimation. There is a recent book [8] that presents basic distributed algorithms for robotic networks. This book shows how tools and notions from different areas such as distributed algorithms, parallel processing, graph theory, computational geometry, control and estimation are used to solve problems of rendezvous, deployment, boundary estimation and tracking.

In this paper, we address the problem of coverage by multi-agent systems—in particular the problem of uniform coverage/sampling. Some representative papers that deal with the problem of coverage/sampling are [9–14]. The term 'coverage' can mean slightly different things to different authors. For example, in [9–12], 'coverage' is more a static concept. i.e., it is a measure of how a static configuration of agents covers a domain or samples a probability distribution. In these papers, the problem is that of redeployment. i.e., given the initial positions of the agents, how do we control the motion of the agents so that they converge to an optimal stationary location? These final stationary agent locations are optimal in the sense that they maximize the detection probability of some event.

* Corresponding author.
E-mail addresses: geoggyreadsmail@gmail.com (G. Mathew), mezic@engineering.ucsb.edu (I. Mezić).

0167-2789/$ – see front matter © 2010 Elsevier B.V. All rights reserved.
doi:10.1016/j.physd.2010.10.010

In [13,14], the term 'coverage' is more of a dynamic concept and is a measure of how well the points on the trajectories of the agents cover a domain. That is, coverage gets better and better as every point in the domain is visited or is close to being visited by an agent. In [13], the authors discuss algorithms for optimal data collection. They discuss an example of a fleet of underwater gliders that move with ocean currents and sample various dynamic oceanographic signals. In [14], the authors study the problem of dynamically covering a region using mobile agents. The notion of coverage we use in this paper is closer to that in [13,14]. Moreover, we use the notion of 'uniform coverage'. In this paper, by 'uniform coverage', we roughly mean that points on the agent trajectories must be as uniformly distributed or evenly spaced throughout the domain.

One approach to achieve uniform coverage is to use lawnmower type strategies (see [15]). In a lawnmower strategy, the area to be covered will be partitioned into equally sized areas and each agent will be assigned to a partition. Then each agent will systemically scan the partition assigned to it by going back and forth in parallel lines. The problems with a lawnmower type approach are:

- It is not straightforward to implement for irregular domains.
- It is not robust to uncertainties (e.g. if one or more of the agents fail, then it is not straightforward for the other agents to adapt accordingly.)
- It is not naturally multiscale. A good uniform coverage algorithm should detect large scale features first, followed by smaller and smaller features.
- It is also not easy to design lawnmower type trajectories to sample non-uniform probability distributions.

The algorithm we present in this paper overcomes all the drawbacks of a lawnmower algorithm that are mentioned above. It can be easily implemented for irregular domains and non-uniform probability distributions. Since our algorithm is based on feedback control laws, it can deal with uncertainties like the failure of one or more of the agents. Also, our algorithm is guaranteed to be multiscale due to the novel metric we use to quantify the uniformity of coverage. The metric we use to quantify the uniformity of coverage was inspired by our previous work to quantify the degree of mixedness of material in a fluid medium (see [16,17]). The notion of uniform coverage can be related to concepts in ergodic theory that relate time averages of functions along trajectories to the spatial averages of functions.

There are many applications of mobile multi-agent systems where it is useful to design their dynamics so that their trajectories are as uniformly distributed as possible in the domain of interest. A couple of scenarios where it is useful to have such dynamics are:

1. *Ocean sampling*: As described in [3,7,13], design of autonomous ocean-sampling networks is an active area of research. The central objective in these projects is to collect data that best reveals the ocean processes and dynamics. They use fleets of underwater gliders in the ocean that take measurements of various oceanographic fields like temperature, salinity and flow. To estimate the state of the ocean at all spatial scales, it is useful that the trajectories of the gliders are as uniformly distributed so that spatial averages of the oceanographic fields can be estimated accurately and efficiently.
2. *Target detection*: For military applications and search-and-rescue operations, target detection using audio/video signals is an important task. For such tasks, it is desirable that there is little space between the trajectories of the mobile sensors so that it becomes difficult for a target to evade detection by the sensors. Of particular interest is the problem of minimizing the time for target detection when the sensor range is very small compared to the domain size and in the presence of uncertainty in terrain and sensor observations. It has been demonstrated that in the presence of uncertainty, uniform coverage based search strategies outperform lawnmower-type search strategies (see [15]).

The rest of the paper is structured as follows. In Section 2, we present the metric that quantifies how far a set of trajectories are from being ergodic. It is this metric that we use to quantify uniform coverage. In Section 3, we use this metric to design dynamics (or feedback control) for multi-agent systems that move according to either first-order dynamics or second-order dynamics. We numerically analyze the behavior of the closed-loop dynamics for various scenarios. The algorithm presented in this paper for the design of ergodic dynamics will be referred to as Spectral Multiscale Coverage (SMC).

2. Metrics for ergodicity (or uniformity of trajectories)

There are N mobile agents and we assume that they move either by first-order or second-order dynamics. We need an appropriate metric to quantify how well the trajectories are sampling a given probability distribution μ. We assume that μ is zero outside a rectangular domain $U \subset \mathbb{R}^n$ and that the agent trajectories are confined to the domain U. For a dynamical system to be ergodic, we know that the fraction of the time spent by a trajectory in a subset must be equal to the measure of the set. Let $B(x, r) = \{y : \|y - x\| \leq r\}$ be a spherical set and $\chi_{(x,r)}$ be the indicator function corresponding to the set $B(x, r)$. Given trajectories $x_j : [0, t] \to \mathbb{R}^n$, for $j = 1, 2, \ldots, N$, the fraction of the time spent by the agents in the set $B(x, r)$ is given as

$$d^t(x, r) = \frac{1}{Nt} \sum_{j=1}^{N} \int_0^t \chi_{(x,r)}(x_j(\tau)) \mathrm{d}\tau.^{2} \tag{1}$$

The measure of the set $B(x, r)$ is given as

$$\bar{\mu}(x, r) = \int_U \mu(y) \chi_{(x,r)}(y) \mathrm{d}y. \tag{2}$$

For ergodic dynamics (see [1]), we must have

$$\lim_{t \to \infty} d^t(x, r) = \bar{\mu}(x, r). \tag{3}$$

Since the equality above must be true for almost all points x and for all radii r, this motivates defining the metric

$$E^2(t) = \int_0^R \int_U (d^t(x, r) - \bar{\mu}(x, r))^2 \mathrm{d}x\mathrm{d}r, \quad \text{where } R > 0. \tag{4}$$

The exact value of the upper limit for the integration of r is not important and does not affect any of the results we present in this paper. $E(t)$ is a metric that quantifies how far the time-averages of indicator functions on spherical sets are from being equal to their spatial averages. Equivalently, it quantifies how far the fraction of the time spent by the agents in spherical sets is from being equal to the measure of the spherical sets. Now consider the distribution C^t defined as[3]

$$C^t(x) = \frac{1}{Nt} \sum_{j=1}^{N} \int_0^t \delta(x - x_j(\tau)) \mathrm{d}\tau. \tag{5}$$

[2] For spheres $B(x, r)$ that lie entirely within the rectangular domain U, the fraction $d^t(x, r)$ is computed as in (1). For spheres $B(x, r)$ that do not lie entirely within the domain U, $d^t(x, r)$ is computed as if each agent trajectory has mirror images about the boundaries of the domain U. Equivalently $d^t(x, r)$ is computed as the spherical integral of the even extension of the distribution C^t defined in (5). See Appendix A for more details.

[3] Strictly speaking, C^t is a distribution and cannot be defined pointwise as a function of x. However, with conventional abuse of notation, we express C^t in terms of the Dirac delta distribution $\delta(.)$ as if it were a function.

Please cite this article in press as: G. Mathew, I. Mezić, Metrics for ergodicity and design of ergodic dynamics for multi-agent systems, Physica D (2010), doi:10.1016/j.physd.2010.10.010

$\delta(.)$ is the Dirac delta distribution. The usual inner product (with respect to the Lebesgue measure) of C^t with a bounded function f is given as

$$\langle C^t, f\rangle = \frac{1}{Nt}\sum_{j=1}^{N}\int_0^t f(x_j(\tau))\mathrm{d}\tau = \frac{1}{Nt}\int_0^t \sum_{j=1}^{N} f(x_j(\tau))\mathrm{d}\tau. \tag{6}$$

Note that the distribution C^t can be thought of as a probability distribution because we have

$$\langle C^t, 1\rangle = \frac{1}{Nt}\sum_{j=1}^{N}\int_0^t 1\mathrm{d}\tau = \frac{Nt}{Nt} = 1. \tag{7}$$

Also note that we have

$$d^t(x, r) = \langle C^t, \chi_{(x,r)}\rangle. \tag{8}$$

Let f_k be the Fourier basis functions that satisfy Neumann boundary conditions on the rectangular domain U and k is the corresponding wave-number vector. For instance, on a rectangular domain $U = [0, L_1]\times[0, L_2]$, we have,

$$\begin{aligned} &f_k(x) = \frac{1}{h_k}\cos(k_1x_1)\cos(k_2x_2), \quad \text{where}\\ &k_1 = \frac{K_1\pi}{L_1} \quad \text{and} \quad k_2 = \frac{K_2\pi}{L_2},\\ &\quad \text{for } K_1, K_2 = 0, 1, 2, \ldots \text{ and where}\\ &h_k = \left(\int_0^{L_1}\int_0^{L_2}\cos^2(k_1x_1)\cos^2(k_2x_2)\mathrm{d}x_1\mathrm{d}x_2\right)^{1/2}, \end{aligned} \tag{9}$$

The division by the factor h_k ensures that f_k has L^2 norm equal to one. Therefore f_k is an orthonormal basis. Now, computing the Fourier coefficients of the distribution C^t, we have

$$c_k(t) = \langle C^t, f_k\rangle = \frac{1}{Nt}\sum_{j=1}^{N}\int_0^t f_k(x_j(\tau))\mathrm{d}\tau. \tag{10}$$

The Fourier coefficients of μ are given as

$$\mu_k = \langle \mu, f_k\rangle. \tag{11}$$

Let $\phi(t)$ be the distance between C^t and μ as given by the Sobolev space norm of negative index (H^{-s}, for $s = \frac{(n+1)}{2}$ and where n is the dimension of the space). i.e.,

$$\begin{aligned} &\phi^2(t) = \|C^t - \mu\|^2_{H^{-s}} = \sum_{K\in\mathbb{Z}^{*n}} \Lambda_k|s_k(t)|^2,\\ &\text{where } s_k(t) = c_k(t) - \mu_k,\ \Lambda_k = \frac{1}{(1+\|k\|^2)^s}\\ &\text{and } \mathbb{Z}^{*n} = [0, 1, 2, \ldots]^n. \end{aligned} \tag{12}$$

Requiring $\phi^2(t)$ to converge to zero is the same as requiring time-averages of the Fourier basis functions along trajectories to converge to the spatial averages of the basis functions. In other words $\phi^2(t)$ quantifies how much the time averages of the Fourier basis functions deviate from their spatial averages, but with more importance given to large-scale modes than the small-scale modes. A related metric to capture deviation from ergodicity that uses wavelet basis functions is described in [18]. The metrics defined above were motivated by our previous work in [16,17] to quantify mixing in fluid flows or the degree of uniformity of material distributed throughout a domain. It can be shown that the two metrics $E(t)$ and $\phi(t)$ are equivalent, i.e., there exist bounded constants such that

$$c_1\phi^2(t) \le E^2(t) \le c_2\phi^2(t). \tag{13}$$

For a proof on the equivalence of these two metrics, see Appendix A. In the rest of the paper, we will be using $\phi^2(t)$ as the metric for uniform coverage (or ergodicity).

3. Design of ergodic dynamics: Spectral Multiscale Coverage (SMC)

The agents move either by first-order or second-order dynamics. First-order dynamics is described by,

$$\dot{x}_j(t) = u_j(t), \tag{14}$$

and second-order dynamics is described by

$$\ddot{x}_j(t) = u_j(t). \tag{15}$$

The objective is to design feedback laws $u_j(t) = F_j(x)$ so that the agents have ergodic dynamics. We do this by designing the feedback so that the metric for uniform coverage ($\phi^2(t)$) is driven to zero. We formulate a model predictive control (or receding horizon control) problem where we try to maximize the rate of decay of the coverage metric at the end of a short time horizon. In receding horizon control, the current control action is chosen by solving a finite horizon optimal control problem. The solution to the optimization problem gives an optimal control solution and the value of the optimal control at the beginning of the horizon is used at the current time. This procedure is repeated at every time instant. The term 'receding horizon' comes from the fact that the horizon recedes ahead in time after each time instant. In our approach here, we derive the feedback law in the limit as the size of the receding horizon goes to zero and use the resulting feedback law at every time instant. For notational convenience, let us define the quantities

$$\begin{aligned} &C_k(t) := \sum_{j=1}^{N}\int_0^t f_k(x_j(\tau))\mathrm{d}\tau = Ntc_k(t)\\ &M_k(t) := Nt\mu_k\\ &S_k(t) := C_k(t) - M_k(t) = Nts_k(t)\\ &\text{and } \Phi(t) := \frac{1}{2}\sum_K \Lambda_k|S_k(t)|^2 = \frac{1}{2}N^2t^2\phi^2(t). \end{aligned} \tag{16}$$

The following limits are useful in our discussions.

$$\begin{aligned} s_k(0) &:= \lim_{t\to 0} s_k(t) = \left(\lim_{t\to 0}\frac{\sum_{j=1}^{N}\int_0^t f_k(x_j(\tau))\mathrm{d}\tau}{Nt} - \mu_k\right)\\ &= \frac{\sum_{j=1}^{N} f_k(x_j(0))}{N} - \mu_k. \quad \text{(by L'Hospital's rule).} \end{aligned} \tag{17}$$

And it follows that

$$\phi^2(0) := \lim_{t\to 0}\phi^2(t) = \sum_K \Lambda_k\left|\frac{\sum_{j=1}^{N} f_k(x_j(0))}{N} - \mu_k\right|^2. \tag{18}$$

3.1. First-order dynamics

Let us introduce the additional variables $W_k(t) := \dot{S}_k(t)$. The dynamics of the extended system which includes the positions of the agents and the variables $S_k(t)$ and $W_k(t)$ can be described as

$$\begin{aligned} &\dot{x}_j(\tau) = u_j(\tau)\\ &\dot{S}_k(\tau) = W_k(\tau) = \sum_{j=1}^{N} f_k(x_j(\tau)) - N\mu_k\\ &\dot{W}_k(\tau) = \sum_{j=1}^{N}\nabla f_k(x_j(\tau))\cdot u_j(\tau). \end{aligned} \tag{19}$$

$\nabla f_k(.)$ is the gradient vector field of the basis functions f_k. For the

Please cite this article in press as: G. Mathew, I. Mezić, Metrics for ergodicity and design of ergodic dynamics for multi-agent systems, Physica D (2010), doi:10.1016/j.physd.2010.10.010

basis functions with Neumann boundary conditions as in (9), we have

$$\nabla f_k(x) = \frac{1}{h_k}\begin{bmatrix} -k_1 \sin(k_1 x_1)\cos(k_2 x_2) \\ -k_2 \cos(k_1 x_1)\sin(k_2 x_2) \end{bmatrix}. \tag{20}$$

At a given time t, let us solve the optimal control problem over the time horizon $[t, t+\Delta t]$. The cost-function we are going to use is the first time-derivative of $\Phi(\tau)$ at the end of the horizon. i.e., we aim to drive the agents to positions which lead to the highest rate of decay of the coverage metric. Also note that minimizing the first time-derivatives of $\phi^2(t)$ and $\Phi(t)$ leads to the same optimal control solutions. The cost-function that we want to minimize is given as

$$C(t, \Delta t) = \dot{\Phi}(t+\Delta t) = \sum_K \Lambda_k S_k(t+\Delta t) W_k(t+\Delta t). \tag{21}$$

The controls are subject to the constraint $\|u_j(\tau)\|_2 \leq u_{\max}$. It is convenient to write the optimal control solution in terms of the costates (Lagrange multipliers) and the Hamiltonian. The dynamics of the costates are given by the costate equations and the Hamiltonian is a function of the states, costates and the controls. The optimal control solution $u_j^*(\tau)$ is the value of an admissible control $u_j(\tau)$ that minimizes the Hamiltonian. For more details on how to form the Hamiltonian and costate equations when solving optimal control problems see [19]. In our notation the costates are $\gamma_j(\tau) \in \mathbb{R}^n$ and $\rho_k(\tau), \sigma_k(\tau) \in \mathbb{R}$ for all K. For our particular problem, the Hamiltonian[4] takes the form

$$\begin{aligned} H(x, S, W, u, \tau) &= \sum_{j=1}^N \gamma_j(\tau)\cdot u_j(\tau) + \sum_K \rho_k(\tau) W_k(\tau) \\ &\quad + \sum_K \sigma_k(\tau)\left(\sum_{j=1}^N \nabla f_k(x_j(\tau))\cdot u_j(\tau)\right). \end{aligned} \tag{22}$$

Now the dynamics for the costates are given as

$$\begin{aligned} \dot{\gamma}_j(\tau) &= -\frac{\partial H}{\partial x_j} = -\sum_K \sigma_k(\tau)(\nabla^2 f_k(x_j(\tau)) u_j(\tau)), \\ \dot{\rho}_k(\tau) &= -\frac{\partial H}{\partial S_k} = 0, \\ \dot{\sigma}_k(\tau) &= -\frac{\partial H}{\partial W_k} = -\rho_k(\tau). \end{aligned} \tag{23}$$

$\nabla^2 f_k(.)$ is the Hessian matrix of the basis functions. The terminal conditions for the costates are given as

$$\begin{aligned} &\gamma_j(t+\Delta t) = 0, \\ &\rho_k(t+\Delta t) = \Lambda_k W_k(t+\Delta t), \\ &\sigma_k(t+\Delta t) = \Lambda_k S_k(t+\Delta t). \end{aligned} \tag{24}$$

The optimal controls u_j^* are such that

$$\begin{aligned} u_j^*(\tau) &= \arg\min_{\|u_j(\tau)\|_2 \leq u_{\max}} H(x, S, W, u, \tau) \\ &= -u_{\max}\frac{\beta_j(\tau)}{\|\beta_j(\tau)\|_2}, \quad \text{if } \beta_j(\tau) \neq 0, \end{aligned} \tag{25}$$

and where $\beta_j(\tau) = \gamma_j(\tau) + \sum_K \sigma_k(\tau)\nabla f_k(x_j(\tau))$.

It can be shown by basic calculus arguments (see Appendix B.1) that in the limit as Δt goes to zero, $u_j^*(t)$ is given as

$$\begin{aligned} &u_j^*(t) = -u_{\max}\frac{B_j(t)}{\|B_j(t)\|_2}, \quad \text{if } B_j(t) \neq 0, \\ &\text{where } B_j(t) = \left[\sum_K \Lambda_k S_k(t)\nabla f_k(x_j(t))\right]. \end{aligned} \tag{26}$$

This is the feedback law we will use to achieve ergodic dynamics.

3.1.1. Alternative interpretation of the control design

The problem of choosing the controls $u_j(t)$ at time t such that it minimizes $\phi(t+\mathrm{d}t)$ for some small $\mathrm{d}t$ is the same as that of minimizing $\Phi(t+\mathrm{d}t)$. Assuming continuity of $u_j(.)$, from basic calculus, we know that

$$\Phi(t+\mathrm{d}t) \approx \Phi(t) + \dot{\Phi}(t)\mathrm{d}t + \frac{1}{2}\ddot{\Phi}(t)\mathrm{d}t^2 =: \widetilde{\Phi}(t, \mathrm{d}t). \tag{27}$$

Now, the first time-derivative of $\Phi(t)$ is given as

$$\dot{\Phi}(t) = \sum_K \Lambda_k S_k(t) W_k(t). \tag{28}$$

Note that since the cost-function $\Phi(t)$ involves time-integrals of functions of agent positions, the current values for the controls $(u_j(t))$ do not directly influence the current value for the first time-derivative $\dot{\Phi}(t)$. But of course, the choice of the controls $u_j(t)$ at the current time can affect the value for the first time-derivative $\dot{\Phi}(t)$ at a later time. Now, the second time-derivative of $\Phi(t)$ is given as

$$\ddot{\Phi}(t) = \sum_K \Lambda_k (W_k(t))^2 + \sum_K \Lambda_k S_k(t)\dot{W}_k(t). \tag{29}$$

Substituting the expression for the derivatives of W_k in the expression for $\ddot{\Phi}$, we get

$$\begin{aligned} \ddot{\Phi}(t) &= \sum_K \Lambda_k (W_k(t))^2 + \sum_K \Lambda_k S_k(t)\left[\sum_{j=1}^N \nabla f_k(x_j(t))\cdot u_j(t)\right] \\ &= \sum_K \Lambda_k (W_k(t))^2 + \sum_{j=1}^N B_j(t)\cdot u_j(t), \end{aligned} \tag{30}$$

where $B_j(t)$ is as defined in (26). Clearly, the choice of $u_j(t)$ that minimizes $\widetilde{\Phi}(t, \mathrm{d}t)$ subject to the constraint $\|u_j(t)\|_2 \leq u_{\max}$ is

$$u_j^*(t) = -u_{\max}\frac{B_j(t)}{\|B_j(t)\|_2}. \tag{31}$$

In other words, the above choice of the feedback law minimizes the second time-derivative of Φ subject to the constraint $\|u_j(t)\|_2 \leq u_{\max}$. It can be shown that

$$\begin{aligned} &\lim_{t\to 0} u_j^*(t) = -u_{\max}\frac{b_j(0)}{\|b_j(0)\|_2}, \\ &\text{where } b_j(0) = \left[\sum_K \Lambda_k s_k(0)\nabla f_k(x_j(0))\right], \end{aligned} \tag{32}$$

and $s_k(0)$ is as defined in (17).

3.1.2. Simulation

In our first example, the objective is to uniformly cover a square domain excluding some regions represented as shaded regions in Fig. 1. Such a situation arises in problems of surveillance by mobile sensor networks. In such a scenario, the shaded regions can be thought of as areas where no sensor measurements can be made due to foliage and therefore there is no value in the sensors spending time over these regions. The target probability distribution μ is set up as follows. First, we define a terrain function as:

$$\mathrm{Ter}(x) = \begin{cases} 1, & \text{if } x \text{ is outside foliage} \\ 0, & \text{if } x \text{ is inside foliage.} \end{cases} \tag{33}$$

[4] For convenience, in our notation we suppress the dependence of the Hamiltonian on the costates.

Please cite this article in press as: G. Mathew, I. Mezić, Metrics for ergodicity and design of ergodic dynamics for multi-agent systems, Physica D (2010), doi:10.1016/j.physd.2010.10.010

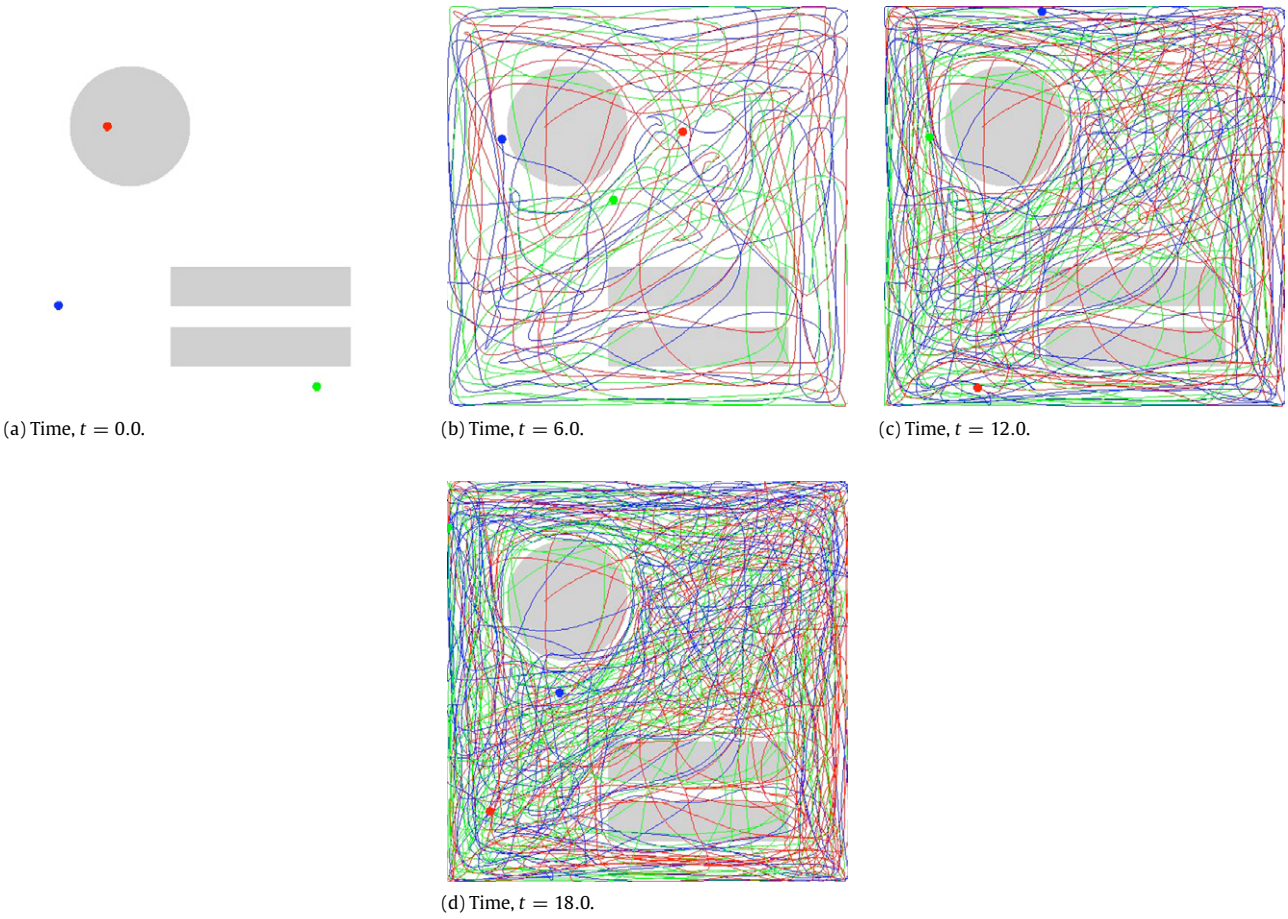

(a) Time, $t = 0.0$. (b) Time, $t = 6.0$. (c) Time, $t = 12.0$. (d) Time, $t = 18.0$.

Fig. 1. Snapshots at various times of the agent trajectories generated by the SMC algorithm with first-order dynamics. One can observe the multiscale nature of the algorithm. The spacing between the trajectories becomes smaller and smaller as time proceeds.

Now, μ is defined as

$$\mu(x) = \frac{\mathrm{Ter}(x)}{\int_U \mathrm{Ter}(y)\mathrm{d}y}. \tag{34}$$

The snapshots in Fig. 1 were generated with a simulation of 3 agents and with the feedback law in (26). The domain U is a unit square domain $[0, 1] \times [0, 1]$, the total simulation time is $T = 18$, and $u_{\max} = 5.0$. The basis functions f_k used are as in (9) for $K_1, K_2 = 0, 1, \ldots, 50$.[5] The initial positions of the agents are chosen randomly.

The differential equations for the closed-loop dynamics of the extended system as described by (19) are solved using a fixed time-step 4th order Runge–Kutta method. Note that the Neumann boundary condition of the basis functions f_k guarantees that the velocity component normal to the boundary at the boundaries of the domain is always zero and therefore the agents never escape the domain.

From the snapshots in Fig. 1, one can see the multiscale nature of the algorithm. The spacing between the trajectories becomes smaller and smaller as time proceeds. One should note that the trajectories are not such that they completely avoid going over the foliage regions as in collision avoidance. Rather, the algorithm generates trajectories such that the fraction of the time spent over the foliage regions is close to zero.

Fig. 2 shows a plot of the decay of the coverage metric $\phi^2(t)$ with time. The decay is not monotonic and in particular for larger times, the decay is irregular. This is partly due to the finite number of basis functions used and the fixed time-stepping used for solving the differential equations. Fig. 2 shows a plot of the fraction of the time spent by the agents outside the foliage regions. It clearly shows that this fraction approaches one, as time proceeds, confirming that the agents spend very little time in the foliage regions. Fig. 3 shows a plot of the norm of the vectors $B_j(t)$. As one can see, although $\|B_j(t)\|_2$ comes close to zero often, it never stays close to zero.

3.2. Second-order dynamics

The dynamics of the extended system that includes the positions and velocities of the agents and the variables $S_k(t)$ and $W_k(t)$ is described as:

$$\begin{aligned} \dot{x}_j(\tau) &= v_j(\tau) \\ \dot{v}_j(\tau) &= u_j(\tau) \\ \dot{S}_k(\tau) &= W_k(\tau) \\ \dot{W}_k(\tau) &= \sum_{j=1}^{N} \nabla f_k(x_j(\tau)) \cdot v_j(\tau). \end{aligned} \tag{35}$$

The forces on the agents are subject to the constraint $\|u_j(\tau)\|_2 \leq F_{\max}$. We are going to use the same model predictive control approach as with first-order dynamics. The cost-function we are going to use here is a weighted sum of the first time-derivative of

[5] For numerical purposes, we need to have a cutoff for the number of Fourier efficients used. The exact effect of this cutoff on the performance of the algorithm is a challenging and interesting problem. Roughly speaking, for a lower cutoff, the gaps left between the trajectories of the agents will be bigger than those obtained with a higher cutoff.

Please cite this article in press as: G. Mathew, I. Mezić, Metrics for ergodicity and design of ergodic dynamics for multi-agent systems, Physica D (2010), doi:10.1016/j.physd.2010.10.010

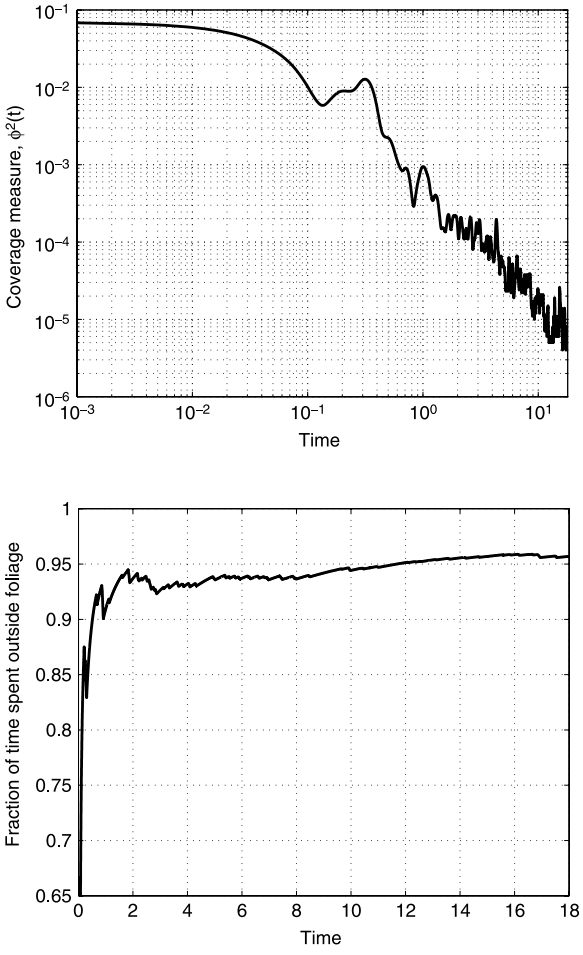

Fig. 2. Results with first-order dynamics: The plot on the top shows the decay of coverage metric $\phi^2(t)$ with time. The decay is not monotonic. The plot on the bottom shows the fraction of the time spent by the agents outside the foliage. This fraction gets closer and closer to one as time proceeds.

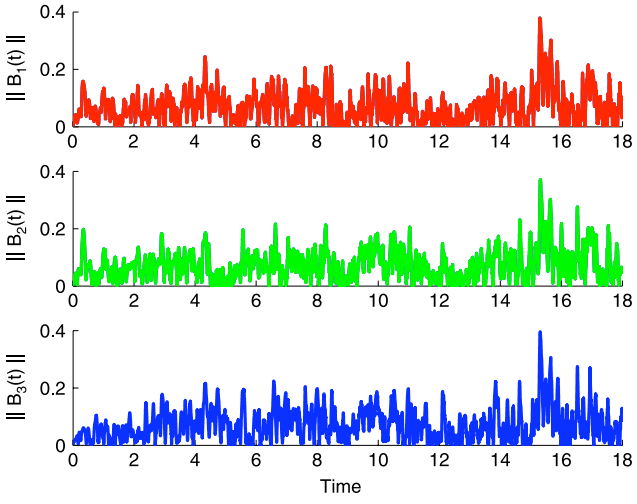

Fig. 3. Results with first-order dynamics: The plot shows the norm of the vectors $B_j(t)$ defined in (26). As one can see, $\|B_j\|_2$, comes close to zero often, but never remains identically close to zero.

$\Phi(\tau)$ and the time-integral of the kinetic energy of the agents. i.e.,

$$C(t, \Delta t) = \dot{\Phi}(t + \Delta t) + \frac{c}{2} \int_t^{t+\Delta t} \sum_{j=1}^{N} v_j(\tau) \cdot v_j(\tau) \mathrm{d}\tau$$

$$= \sum_K \Lambda_k S_k(t + \Delta t) W_k(t + \Delta t) + \frac{c}{2} \int_t^{t+\Delta t} \sum_{j=1}^{N} v_j(\tau) \cdot v_j(\tau). \quad (36)$$

In the cost-function, c is a parameter that decides how much the kinetic energy is penalized. The higher the value of c, the lower will be the resulting velocities of the agents. Let $\alpha_j(\tau) \in \mathbb{R}^n$, $\beta_j(\tau) \in \mathbb{R}^n$ and $\rho_k(\tau)$, $\sigma_k(t) \in \mathbb{R}$ for all K be the costates. Then the Hamiltonian takes the form

$$H(x, v, S, W, u, \tau) = \frac{c}{2} \sum_{j=1}^{N} v_j(\tau) \cdot v_j(\tau) + \sum_{j=1}^{N} \alpha_j(\tau) \cdot v_j(\tau) + \sum_{j=1}^{N} \beta_j(\tau) \cdot u_j(\tau) + \sum_K \rho_k(\tau) W_k(\tau) + \sum_K \sigma_k(\tau) \left(\sum_{j=1}^{N} \nabla f_k(x_j(\tau)) \cdot v_j(\tau) \right). \quad (37)$$

Now the costate equations are given as

$$\begin{aligned} \dot{\alpha}_j(\tau) &= -\frac{\partial H}{\partial x_j} = -\sum_K \sigma_k(\tau) \left(\nabla^2 f_k(x_j(\tau)) v_j(\tau) \right), \\ \dot{\beta}_j(\tau) &= -\frac{\partial H}{\partial v_j} = -c v_j(\tau) - \alpha_j(\tau) - \sum_K \sigma_k(\tau) \nabla f_k(x_j(\tau)), \\ \dot{\rho}_k(\tau) &= -\frac{\partial H}{\partial S_k} = 0, \\ \dot{\sigma}_k(\tau) &= -\frac{\partial H}{\partial W_k} = -\rho_k(\tau). \end{aligned} \quad (38)$$

The terminal constraints are given as

$$\begin{aligned} \alpha_j(t + \Delta t) &= \beta_j(t + \Delta t) = 0, \\ \rho_k(t + \Delta t) &= \Lambda_k W_k(t + \Delta t), \\ \sigma_k(t + \Delta t) &= \Lambda_k S_k(t + \Delta t). \end{aligned} \quad (39)$$

The optimal controls u_j^* are such that

$$u_j^*(\tau) = \arg \min_{\|u_j(\tau)\|_2 \le F_{\max}} H(x, v, S, W, u, \tau) = -F_{\max} \frac{\beta_j(\tau)}{\|\beta_j(\tau)\|_2}, \quad \text{if } \beta_j(\tau) \neq 0. \quad (40)$$

By some basic calculus arguments (see Appendix B.2), we can show that in the limit as Δt goes to zero, we get:

$$u_j^*(t) = -F_{\max} \frac{\left(c v_j(t) + B_j(t) \right)}{\| c v_j(t) + B_j(t) \|_2}, \quad \text{where } B_j(t) = \left[\sum_K \Lambda_k S_k(t) \nabla f_k(x_j(t)) \right]. \quad (41)$$

Another way to interpret the control law in (41) is to see that it is the control law that makes the second time-derivative of $C(0, t)$ as negative as possible. The results shown in Fig. 4 were generated with a simulation of 4 agents, with weighting parameter $c = 0.2$ and $F_{\max} = 50.0$. The total simulation time is $T = 48.0$ and the domain is a unit square as before, but with a different foliage region. The basis functions used are the same as before. The initial positions of the agents are chosen randomly and the initial velocities are zero. (The initial velocities could also be chosen randomly—the algorithm would work the same.) As opposed to first-order dynamics, it is not guaranteed that the agents are always confined in the domain even though the force component normal to the boundaries is zero at the boundary. To resolve this, we force the agents inward toward the domain with maximum force whenever they leave the domain.

Please cite this article in press as: G. Mathew, I. Mezić, Metrics for ergodicity and design of ergodic dynamics for multi-agent systems, Physica D (2010), doi:10.1016/j.physd.2010.10.010

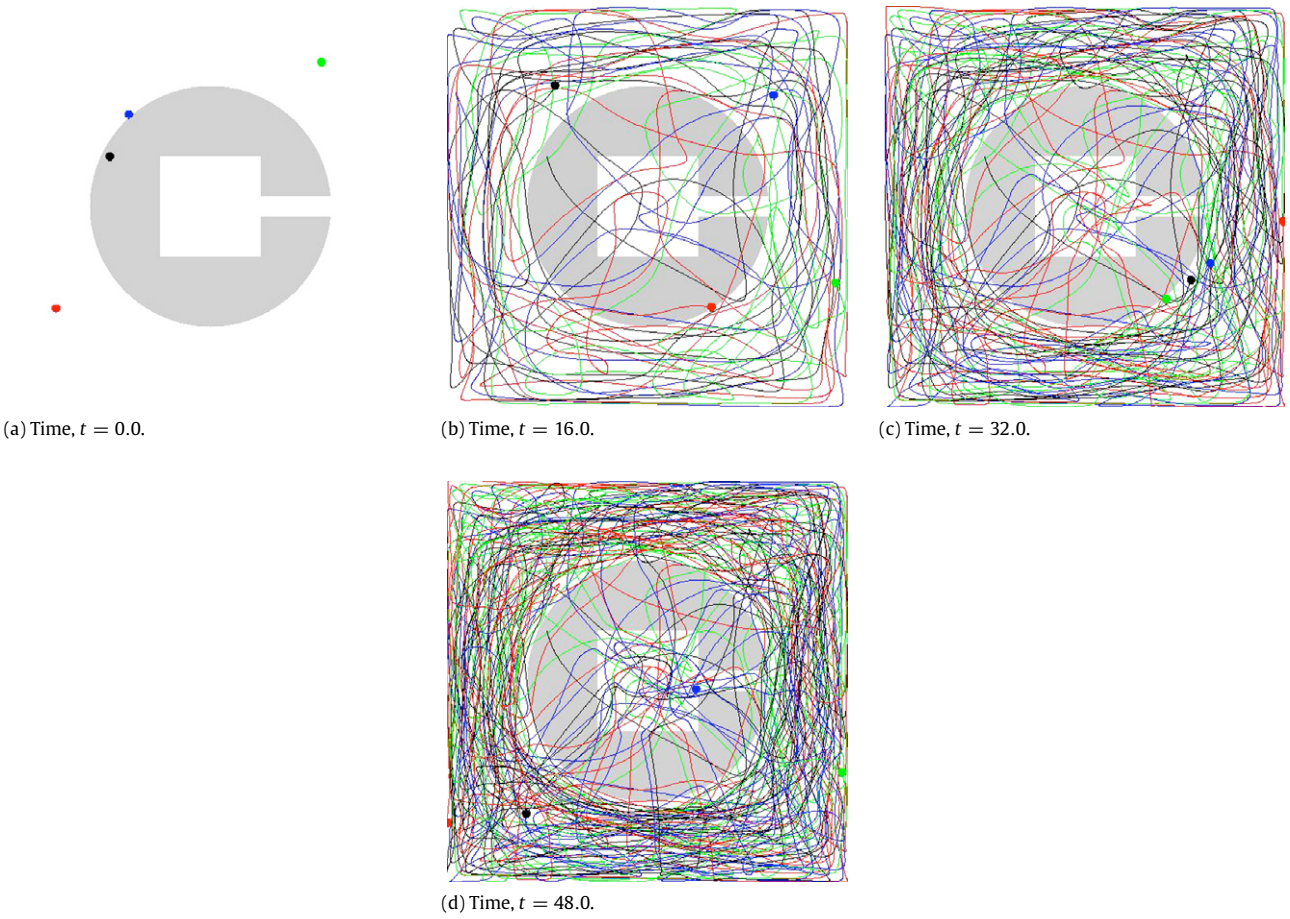

(a) Time, $t = 0.0$. (b) Time, $t = 16.0$. (c) Time, $t = 32.0$.

(d) Time, $t = 48.0$.

Fig. 4. Snapshots at various times of the agent trajectories generated by the SMC algorithm with second-order dynamics.

Fig. 5 shows a plot of the decay of the coverage metric $\phi^2(t)$ with time. The initial rate of decay is small because the initial velocities of the agents are zero and it takes some time for them to start moving at a reasonable velocity. Fig. 5 also shows a plot of the fraction of the time spent by the agents outside the foliage regions. Fig. 6 shows a plot of the norm of the vectors $B_j(t)$ and as before they never stay close to zero.

3.3. Remarks on convergence

Spatial averages of functions can be estimated by computing the time averages of functions along trajectories generated by the SMC algorithm. Given a test function f, its spatial average can be estimated as

$$\bar{f}(t) = \frac{1}{Nt} \sum_{j=1}^{N} \int_0^t f(x_j(\tau)) \mathrm{d}\tau. \tag{42}$$

Then the sampling error at time t is computed as

$$e(t) = |\bar{f}(t) - \langle \mu, f \rangle|. \tag{43}$$

To study the convergence of the sampling error, we are going to assume a uniform prior on the unit square domain and use the test function

$$f(x) = x_1^2 + x_2^2. \tag{44}$$

Figs. 7 and 8 show the sampling error as a function of time with trajectories generated by the SMC algorithm with first-order dynamics and second-order dynamics respectively. The different lines correspond to various values of N (number of agents). The plots shown in Figs. 7 and 8 are error curves averaged over 100 different realizations and are shown on a log–log scale. These plots indicate that the sampling error is roughly $O(t^{-1})$. This is similar to quasi-Monte Carlo sampling which has error $O(t^{-1})$ as opposed to regular Monte Carlo sampling which has error $O(t^{-1/2})$. (Here of course, time t plays the role of number of samples.) This is not surprising because quasi-Monte Carlo methods are based on low-discrepancy sequences and similarly the SMC algorithm attempts to generate points on agent trajectories such that they have uniform density throughout the domain. Recall that the discrepancy of a sequence is said to be low if the number of points in the sequence falling in a arbitary set B is almost proportional to the measure of the set B. Therefore, the coverage metrics ($E(t)$ and $\phi(t)$) can also be interpreted as metrics for the discrepancy of the points on the agent trajectories and the SMC algorithm is constantly attempting to reduce this discrepancy.

To understand the $O(t^{-1})$ convergence, it is helpful to look closer at the dynamics of the S_k and W_k variables with the feedback control as described in the previous sections. Fig. 9 shows the evolution of the vector $(S_k(t), W_k(t))$ under the closed-loop first-order dynamics for different values of K. As one can see, the variables $S_k(t)$ and $W_k(t)$ exhibit oscillatory dynamics and appear to remain bounded at all times. If $S_k(t)$ remains bounded for all times, it follows that $|s_k(t)|$ is $O(t^{-1})$ and therefore the sampling error corresponding to a test function f which can be represented as a finite combination of Fourier modes would be $O(t^{-1})$. However, proving that $S_k(t)$ for all K remains bounded at all times is a challenging problem and will be the subject of future work.

Please cite this article in press as: G. Mathew, I. Mezić, Metrics for ergodicity and design of ergodic dynamics for multi-agent systems, Physica D (2010), doi:10.1016/j.physd.2010.10.010

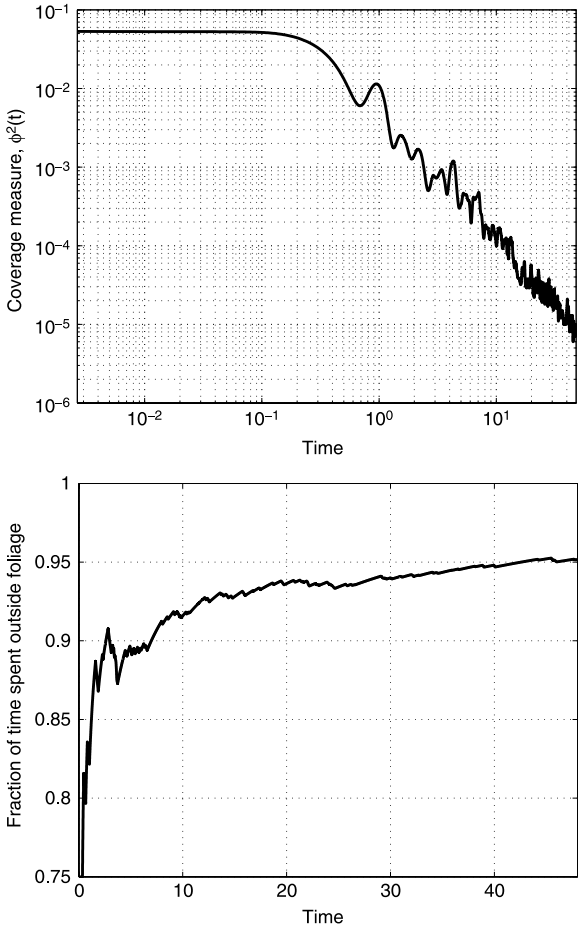

Fig. 5. Results with second-order dynamics: The plot on the top shows decay of coverage metric $\phi^2(t)$ with time. Decay is not monotonic. The initial rate of decay is small because the initial velocities of the agents are zero and it takes some time for them to start moving at a reasonable velocity. The plot on the bottom shows the fraction of the time spent by the agents outside the foliage. One can see that this fraction gets closer and closer to one as time proceeds.

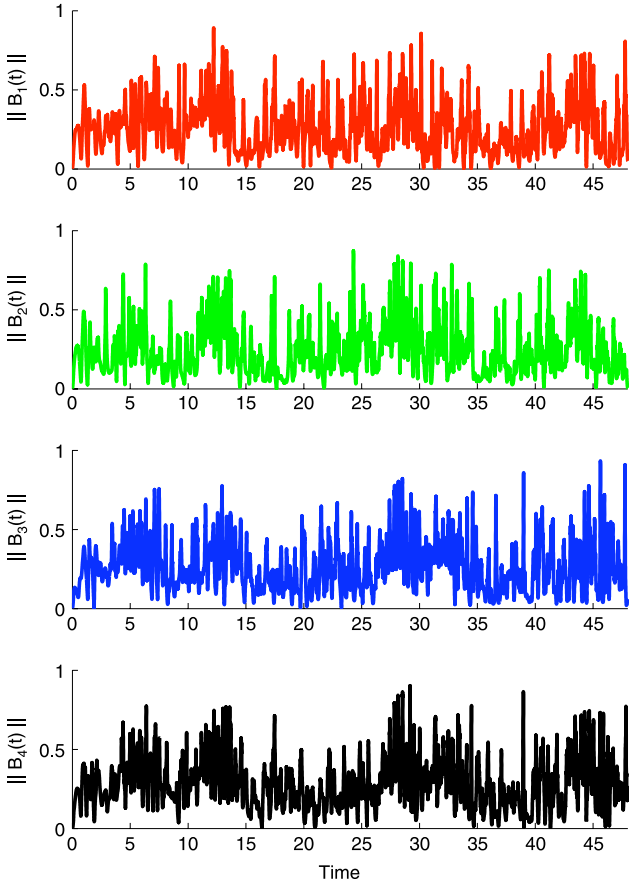

Fig. 6. Results with second-order dynamics: The plot shows the norm of the vectors $B_j(t)$ defined in (41).

4. Discussion

We have proposed centralized feedback control laws for multi-agent systems to achieve uniform coverage of a given domain. The algorithm presented in this paper is fairly easy to implement and more importantly very easy to apply to domains of various geometries. A change in the geometry requires only defining an appropriate terrain function as in (33), computing the corresponding target probability distribution μ and its Fourier coefficients μ_k. Also, for a fixed number of basis functions, the computational complexity of the algorithm is $O(N)$. It must also be noted that the time taken to compute the feedback laws increases linearly with the number of Fourier coefficients used. Therefore it would be useful to develop techniques to compute the feedback laws efficiently.

Various numerical simulations have demonstrated the effectiveness of the algorithm. One could solve the optimal control problem over a non-zero time horizon instead of deriving the feedback law in the limit as the receding horizon goes to zero. But this is a computationally intensive problem. The feedback laws we have derived are remarkably effective while being easy to implement and compute. Proving asymptotic decay of the uniform coverage metric $\phi^2(t)$ with the proposed feedback laws for arbitrary probability distributions μ, remains an open problem. In particular, it needs to be shown that the vector $B_j(t)$ defined in (26) never approaches and stays at zero. However, numerical simulations suggest that this is unlikely. Rigorous proofs for this will be the subject of future work. Future work also includes modifications of the algorithm to achieve decentralization so that the agents can achieve uniform coverage just by local interactions.

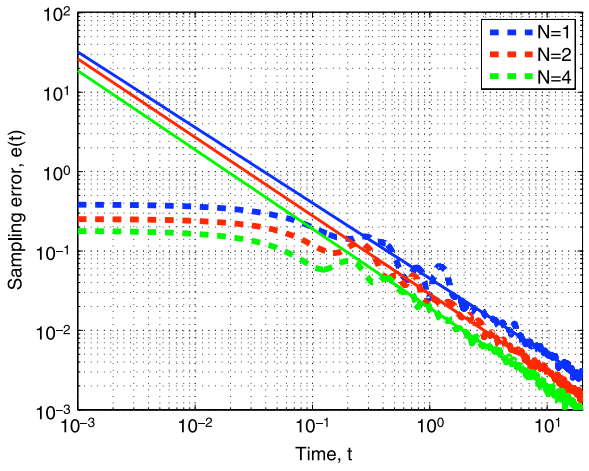

Fig. 7. Results with first-order dynamics: The sampling error $e(t)$ is computed as in (43) and averaged over 100 different realizations. The plots show the averaged sampling error as a function of time on a log–log scale. The dashed curves represent the actual error while the solid lines represent the least squares linear fits to the log–log plots. The negative slopes for the linear fits are 0.9514, 0.9878 and 0.9963 respectively for $N = 1$, $N = 2$ and $N = 4$. This indicates that the error is roughly $O(t^{-1})$.

Please cite this article in press as: G. Mathew, I. Mezić, Metrics for ergodicity and design of ergodic dynamics for multi-agent systems, Physica D (2010), doi:10.1016/j.physd.2010.10.010

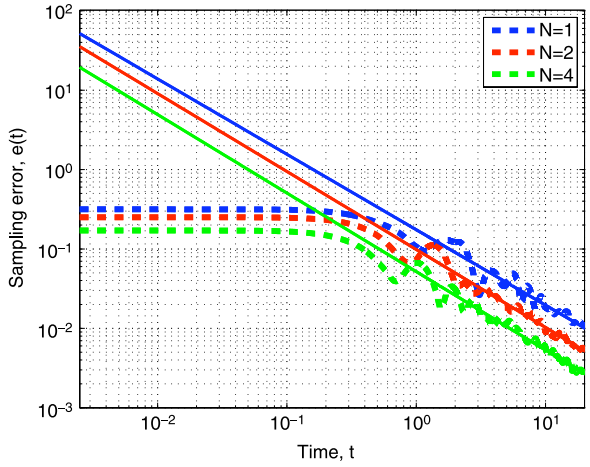

Fig. 8. Results with second-order dynamics: The averaged sampling error $e(t)$ is computed and plotted as described for Fig. 7. The negative slopes for the linear fits are 0.9499, 0.9818 and 0.9890 respectively for $N = 1, N = 2$ and $N = 4$. This indicates that the error is roughly $O(t^{-1})$.

Acknowledgements

This work was supported by the Office of Naval Research (Grant No. N00014-07-1-0587). The first author performed this work as a postdoctoral scholar at the University of California, Santa Barbara and is now an employee of United Technologies Research Center (UTRC), Inc., Berkeley, California.

Appendix A. Multiscale interpretation of the metric for uniformity of trajectories

$U \subset \mathbb{R}^n$ is a rectangular domain given as $[0, L_1] \times [0, L_2] \times \cdots \times [0, L_n]$. Let δ_σ be a delta sequence. i.e. given a bounded function $f : U \to \mathbb{R}$ and for $x_0 \in U$, we have

$$\lim_{\sigma \to 0} \int_U \delta_\sigma (x - x_0) f(x) \mathrm{d}x = f(x_0). \tag{A.1}$$

Let us define the distribution C_σ^t such that for all $x \in U$, we have

$$C_\sigma^t(x) := \frac{1}{Nt} \sum_{j=1}^{N} \int_0^t \delta_\sigma (x - x_j(\tau)) \mathrm{d}\tau. \tag{A.2}$$

It can be seen that for any bounded function f, we have

$$\lim_{\sigma \to 0} \left\langle C_\sigma^t, f \right\rangle = \langle C^t, f \rangle, \tag{A.3}$$

where C^t is as defined in (6). Let f_k be the Fourier basis functions that satisfy Neumann boundary conditions on the rectangular domain U. i.e.,

$$f_k(x) = \frac{1}{h_k} \prod_{i=1}^{n} \cos(k_i x_i), \quad \text{where}$$

$$k_i = \frac{K_i \pi}{L_i} \quad \text{and for } K_i, K_2 = 0, 1, 2, \ldots \text{ and where} \tag{A.4}$$

$$h_k = \left(\int_U \prod_{i=1}^{n} \cos^2(k_i x_i) \, \mathrm{d}x \right)^{1/2}.$$

The division by the factor h_k ensures that f_k is an orthonormal basis. Now let D_σ^t be the even extension of C_σ^t outside the domain U. Equivalently

$$D_\sigma^t(x) = \sum_K c_k^\sigma(t) f_k(x), \tag{A.5}$$

where

$$c_k^\sigma(t) = \langle C_\sigma^t, f_k \rangle. \tag{A.6}$$

Now, we define the integral operator $[I(r)]$ such that

$$[I(r)] C_\sigma^t(x) := \int_{B(x,r)} D_\sigma^t(y) \mathrm{d}y, \quad \text{for all } x \in U \tag{A.7}$$

where $B(x, r) = \{y : \|y - x\| \le r\}$. Given a probability distribution μ, we shall define the following metric:

$$F^2(C_\sigma^t - \mu) := \int_0^R \left(\int_U \left(\int_{B(x,r)} (D_\sigma^t(y) - \mu_e(y)) \mathrm{d}y \right)^2 \mathrm{d}x \right) \mathrm{d}r \tag{A.8}$$

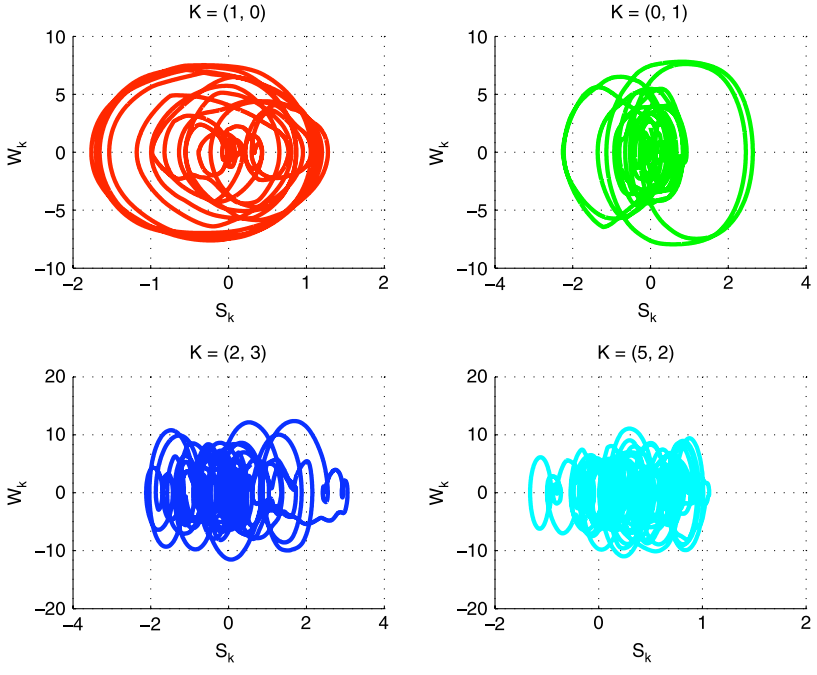

Fig. 9. Evolution of the vector $(S_k(t), W_k(t))$ for different values of K under the SMC algorithm with first-order dynamics. The variables exhibit oscillatory dynamics and remain bounded for all times.

Please cite this article in press as: G. Mathew, I. Mezić, Metrics for ergodicity and design of ergodic dynamics for multi-agent systems, Physica D (2010), doi:10.1016/j.physd.2010.10.010

where μ_e is similarly the even extension of μ. The metric F compares the spherical integrals of the distributions D_σ^t and μ_e. The metric F can be equivalently written as

$$F^2(C_\sigma^t - \mu) = \int_0^R \langle [I(r)](C_\sigma^t - \mu), [I(r)](C_\sigma^t - \mu)\rangle. \tag{A.9}$$

Since we have

$$[I(r)]f_k(x) = i_k(r) f_k(x), \tag{A.10}$$

where $i_k(r)$ is as defined in (A.23), it follows that

$$\begin{aligned} F^2(C_\sigma^t - \mu) &= \int_0^R \left(\sum_K i_k^2(r) \left(c_k^\sigma(t) - \mu_k\right)^2 \right) \mathrm{d}r \\ &= \sum_K a_k \left(c_k^\sigma(t) - \mu_k\right)^2 \end{aligned} \tag{A.11}$$

where $a_k = \int_0^R i_k^2(r)\mathrm{d}r$.

Note that the metric for ergodicity $E(t)$ is given as

$$E^2(t) = \lim_{\sigma \to 0} F^2(C_\sigma^t - \mu), \tag{A.12}$$

because we have

$$\lim_{\sigma \to 0} [I(r)]C_\sigma^t(x) = d^t(x, r), \tag{A.13}$$

where $d^t(x, r)$ is the fraction of the time spent by the agents in the set $B(x, r)$ if $B(x, r) \subset U$. If $B(x, r)$ does not lie entirely within the domain U, $d^t(x, r)$ is the fraction of the time spent by the agents and their mirror images in the set $B(x, r)$. Therefore

$$\begin{aligned} E^2(t) &= \lim_{\sigma \to 0} F^2(C_\sigma^t - \mu) \\ &= \lim_{\sigma \to 0} \sum_K a_k \left(c_k^\sigma(t) - \mu_k\right)^2 \\ &= \sum_K a_k \left(c_k(t) - \mu_k\right)^2, \end{aligned} \tag{A.14}$$

where

$$c_k(t) = \langle C^t, f_k\rangle \quad \text{and} \quad \mu_k = \langle \mu, f_k\rangle. \tag{A.15}$$

Moreover, it can be shown that there exists bounded constants $c_1, c_2 > 0$ such that

$$\begin{aligned} &\frac{c_1}{(1 + \|k\|^2)^s} \le a_k \le \frac{c_2}{(1 + \|k\|^2)^s}, \\ &\text{for } s = \frac{(n+1)}{2}, \end{aligned} \tag{A.16}$$

and where n is the dimension of the space. Thus, we have that

$$c_1 \phi^2(t) \le E^2(t) \le c_2 \phi^2(t) \tag{A.17}$$

where

$$\phi^2(t) = \|C^t - \mu\|_{H^{-s}}^2 = \sum_K \frac{[c_k(t) - \mu_k]^2}{(1 + \|k\|^2)^s}. \tag{A.18}$$

A.1. Proof for inequality (A.16)

f_k is the solution of the Helmholtz equation

$$\Delta f_k + \lambda_k f_k = 0, \tag{A.19}$$

for $\lambda_k = \sum_{i=1}^n k_i^2$. It is well know that solutions of the Helmholtz equation satisfy the following mean value theorem (see [20]).

$$\begin{aligned} [H(r)]f_k(x) &:= \frac{\int_{S(x,r)} f_k(y)\mathrm{d}y}{\mathrm{Area}(S(x, r))} \\ &= \frac{\Gamma\left(\frac{n}{2}\right) J_{(n-2)/2}(r\sqrt{\lambda_k})}{(r\sqrt{\lambda_k}/2)^{(n-2)/2}} f_k(x), \end{aligned} \tag{A.20}$$

where $S(x, r) = \{y : \|y - x\| = r\}$. $J_{(n-2)/2}$ is a Bessel function of the first kind and Γ is the gamma function. Therefore, we have

$$\begin{aligned} [I(r)]f_k(x) &= \int_{B(x,r)} f_k(y)\mathrm{d}y \\ &= \int_0^r [H(s)]f_k(x).\mathrm{Area}(S(x, s))\mathrm{d}s. \end{aligned} \tag{A.21}$$

Using the formula for $\mathrm{Area}(S(x, s)) = \frac{2\pi^{n/2} s^{(n-1)}}{\Gamma\left(\frac{n}{2}\right)}$, we get

$$\begin{aligned} [I(r)]f_k(x) &= \int_0^r \frac{\Gamma\left(\frac{n}{2}\right) J_{(n-2)/2}(s\sqrt{\lambda_k})}{(s\sqrt{\lambda_k}/2)^{(n-2)/2}} f_k(x).\frac{2\pi^{n/2} s^{(n-1)}}{\Gamma\left(\frac{n}{2}\right)}\mathrm{d}s \\ &= \left(\frac{(2\pi)^{n/2}}{(\sqrt{\lambda_k})^{(n-2)/2}} \int_0^r J_{(n-2)/2}\left(s\sqrt{\lambda_k}\right) s^{n/2}\mathrm{d}s \right) f_k(x) \\ &= \left(\frac{(2\pi)^{n/2}}{(\sqrt{\lambda_k})^n} J_{(n/2)}(r\sqrt{\lambda_k})(r\sqrt{\lambda_k})^{n/2} \right) f_k(x), \end{aligned} \tag{A.22}$$

where we use the derivative identity $\mathrm{d}[x^m J_m(x)]/\mathrm{d}x = x^m J_{m-1}(x)$. Therefore

$$\begin{aligned} &[I(r)]f_k(x) = i_k(r).f_k(x), \quad \text{where} \\ &i_k(r) := \left(\frac{(2\pi)^{n/2}}{(\sqrt{\lambda_k})^n} J_{(n/2)}(r\sqrt{\lambda_k})(r\sqrt{\lambda_k})^{n/2} \right). \end{aligned} \tag{A.23}$$

Now we have

$$\begin{aligned} a_k &:= \int_0^R i_k^2(r)\mathrm{d}r = \frac{(2\pi)^n}{(\sqrt{\lambda_k})^{2n}} \int_0^R J_{(n/2)}^2(r\sqrt{\lambda_k})(r\sqrt{\lambda_k})^n \mathrm{d}r \\ &= \frac{(2\pi)^n}{(\sqrt{\lambda_k})^{n+1}} \int_0^R J_{(n/2)}^2(r\sqrt{\lambda_k}) r^n \sqrt{\lambda_k}\mathrm{d}r. \end{aligned} \tag{A.24}$$

Let us define

$$A(\lambda_k) := (2\pi)^n \int_0^R J_{(n/2)}^2(r\sqrt{\lambda_k}) r^n \sqrt{\lambda_k}\mathrm{d}r. \tag{A.25}$$

We have that

$$0 \le A(\lambda_k) \le U \quad \text{for all } k, \tag{A.26}$$

where U is a bounded constant. This follows from noting that

$$\begin{aligned} A(\lambda_k) &\le (2\pi)^n \sqrt{\lambda_k} R^n \int_0^\infty J_{(n/2)}^2(r\sqrt{\lambda_k})\mathrm{d}r, \\ &= (2\pi R)^n \sqrt{\lambda_k} \frac{V}{\sqrt{\lambda_k}} = (2\pi R)^n V = U, \end{aligned} \tag{A.27}$$

where V is a bounded constant that depends only on the dimension of the space. The integral in the above expression follows from Formula 6.512 on Page 666 of [21]. Fig. A.10 shows a plot of $A(\lambda_k)$ as a function of λ_k for $R = 1$ and for $n = 1, 2$ and 3. Thus we have

$$a_k \le \frac{U}{(\lambda_k)^{\frac{n+1}{2}}} \quad \text{for } k \ne 0, \tag{A.28}$$

and for W sufficiently large enough, we have

$$a_k \le \frac{WU}{(1 + \lambda_k)^{\frac{n+1}{2}}} = \frac{c_2}{(1 + \lambda_k)^{\frac{n+1}{2}}}, \quad \text{for all } k. \tag{A.29}$$

Also, for $k \ne 0$, we can choose ϵ small enough so that

Please cite this article in press as: G. Mathew, I. Mezić, Metrics for ergodicity and design of ergodic dynamics for multi-agent systems, Physica D (2010), doi:10.1016/j.physd.2010.10.010

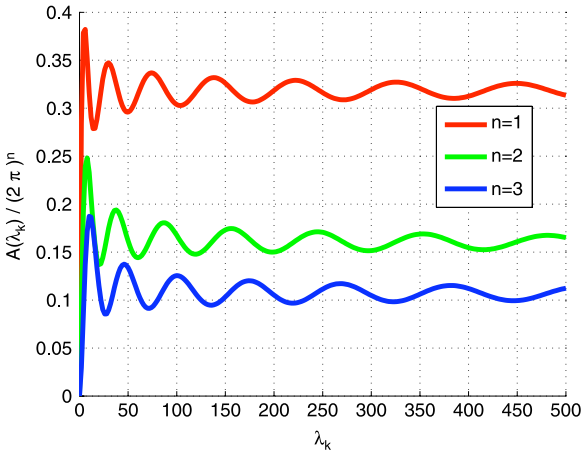

Fig. A.10. Plot of $\frac{A(\lambda_k)}{(2\pi)^n}$ as a function of λ_k.

$$\begin{aligned} a_k &\geq \frac{(2\pi)^n}{(\sqrt{\lambda_k})^{n+1}} \int_0^\epsilon J^2_{(n/2)}(r\sqrt{\lambda_k}) r^n \sqrt{\lambda_k} \mathrm{d}r \\ &\geq \frac{(2\pi)^n}{(1+\lambda_k)^{(n+1)/2}} \int_0^\epsilon J^2_{(n/2)}(r\sqrt{\lambda_k}) r^n \sqrt{\lambda_k} \mathrm{d}r \\ &\geq \frac{\beta_n(\epsilon)}{(1+\lambda_k)^{(n+1)/2}}, \end{aligned} \tag{A.30}$$

where

$$\beta_n(\epsilon) := (2\pi)^n \inf_{K\neq 0} \int_0^\epsilon J^2_{(n/2)}(r\sqrt{\lambda_k}) r^n \sqrt{\lambda_k} \mathrm{d}r. \tag{A.31}$$

Again, we can choose ϵ small enough so that $c_1 = \beta_n(\epsilon) \leq a_0$, giving

$$\frac{c_1}{(1+\lambda_k)^{\frac{n+1}{2}}} \leq a_k, \quad \text{for all } k. \tag{A.32}$$

Appendix B. Solution to model-predictive problem as receding horizon goes to zero

B.1. First-order dynamics

From (23)–(25), we have

$$\begin{aligned} u_j^*(\tau) &= -u_{\max} \frac{\beta_j(\tau)}{\|\beta_j(\tau)\|_2} \\ \text{where } \beta_j(\tau) &= \gamma_j(\tau) + \sum_K \sigma_k(\tau) \nabla f_k(x_j(\tau)). \end{aligned} \tag{B.1}$$

The solutions of the costates γ_j and σ_k at time t up to first-order accuracy in Δt are given as

$$\begin{aligned} \gamma_j(t) &= \gamma_j(t+\Delta t) - \dot\gamma_j(t+\Delta t)\Delta t = -\dot\gamma_j(t+\Delta t)\Delta t, \\ \sigma_k(t) &= \sigma_k(t+\Delta t) - \dot\sigma_k(t+\Delta t)\Delta t \\ &= \Lambda_k S_k(t+\Delta t) + \rho_k(t+\Delta t)\Delta t. \end{aligned} \tag{B.2}$$

From the above expressions, we have $\lim_{\Delta t\to 0} \gamma_j(t) = 0$ and $\lim_{\Delta t\to 0} \sigma_k(t) = \Lambda_k S_k(t)$. Thus we get

$$\lim_{\Delta t\to 0} \beta_j(t) = \sum_K \Lambda_k S_k(t) \nabla f_k(x_j(t)), \tag{B.3}$$

giving the feedback law in (26).

B.2. Second-order dynamics

From (38)–(40), we have

$$u_j^*(\tau) = -F_{\max} \frac{\beta_j(\tau)}{\|\beta_j(\tau)\|_2}. \tag{B.4}$$

The solution of the costate β_j at time t up to first-order accuracy in Δt is given as

$$\begin{aligned} \beta_j(t) &= \beta_j(t+\Delta t) - \dot\beta_j(t+\Delta t)\Delta t \\ &= 0 + \left[c v_j(t+\Delta t) + \alpha_j(t+\Delta t)\right]\Delta t \\ &\quad + \left[\sum_K \sigma_k(t+\Delta t) \nabla f_k(x_j(t+\Delta t))\right]\Delta t. \end{aligned} \tag{B.5}$$

We have $\alpha_j(t+\Delta t) = 0$ and $\lim_{\Delta t\to 0} \sigma_k(t+\Delta t) = \Lambda_k S_k(t)$. Thus we get

$$\begin{aligned} \lim_{\Delta t\to 0} \frac{\beta_j(t)}{\|\beta_j(t)\|_2} &= \frac{c v_j(t) + B_j(t)}{\|c v_j(t) + B_j(t)\|_2} \\ \text{where } B_j(t) &= \left[\sum_K \Lambda_k S_k(t) \nabla f_k(x_j(t))\right]. \end{aligned} \tag{B.6}$$

leading to the feedback law in (41).

References

[1] K. Petersen, Ergodic Theory, Cambridge University Press, 1984.
[2] P.V. y Alvarado, K. Youcef-Toumi, Design of machines with compliant bodies for biomimetic locomotion in liquid environments, J. Dyn. Syst. Meas. Control 128 (1) (2006) 3–13.
[3] E. Fiorelli, N.E. Leonard, P. Bhatta, D.A. Paley, R. Bachmayer, D.M. Fratantoni, Multi-AUV control and adaptive sampling in Monterey bay, IEEE J. Ocean. Eng. 31 (4) (2006) 935–948.
[4] P. Rybski, N. Papanikolopoulos, S. Stoeter, D. Krantz, K. Yesin, M. Gini, R. Voyles, D. Hougen, B. Nelson, M. Erickson, Enlisting rangers and scouts for reconnaissance and surveillance, IEEE Robot. Autom. Mag. 7 (4) (2000) 14–24.
[5] C.A. Rabbath, C.-Y. Su, A. Tsourdos, Guest editorial introduction to the special issue on multivehicle systems cooperative control with application, IEEE Trans. Control Syst. Technol. 15 (4) (2007) 599–600.
[6] F. Bullo, J. Cortés, B. Piccoli, Special issue on control and optimization in cooperative networks, SIAM J. Control Optim. 48 (1) (2009) vii.
[7] T. Curtin, J. Bellingham, Guest editorial—autonomous ocean-sampling networks, IEEE J. Ocean. Eng. 26 (4) (2001) 421–423.
[8] F. Bullo, J. Cortés, S. Martínez, Distributed Control of Robotic Networks, in: Applied Mathematics Series, Princeton University Press, 2009, (electronically). Available at: http://coordinationbook.info.
[9] A. Howard, M.J. Mataric, G.S. Sukhatme, Mobile sensor network deployment using potential fields: a distributed, scalable solution to the area coverage problem, 2002, pp. 299–308.
[10] J. Cortes, S. Martinez, T. Karatas, F. Bullo, Coverage control for mobile sensing networks, IEEE Trans. Robot. Autom. 20 (2) (2004) 243–255.
[11] W. Li, C.G. Cassandras, Distributed cooperative coverage control of sensor networks, in: Proc. of 44th IEEE Conf. on Decision and Control, 2005.
[12] F. Lekien, N.E. Leonard, Nonuniform coverage and cartograms, SIAM J. Control Optim. 48 (1) (2009) 351–372.
[13] N. Leonard, D. Paley, F. Lekien, R. Sepulchre, D. Fratantoni, R. Davis, Collective motion, sensor networks, and ocean sampling, Proc. IEEE 95 (1) (2007) 48–74.
[14] I. Hussein, D. Stipanović, Effective coverage control for mobile sensor networks with guaranteed collision avoidance, in: Multi-Vehicle Systems Cooperative Control with Applications, IEEE Trans. Control Syst. Technol. 15 (4) (2007) 642–657. (special issue).
[15] A. Hubenko, V.A. Fonoberov, G. Mathew, I. Mezic, Multiscale adaptive search, IEEE Trans. Syst. Man Cybern. B (2010) (in press).
[16] G. Mathew, I. Mezic, L. Petzold, A multiscale measure for mixing, Physica D 211 (2005) 23–46.
[17] G. Mathew, I. Mezic, S. Grivopoulos, U. Vaidya, L. Petzold, Optimal control of mixing in stokes fluid flows, J. Fluid Mech. 580 (2007) 261–281.
[18] S.E. Scott, T.C. Redd, L. Kuznetsov, I. Mezic, C.K. Jones, Capturing deviation from ergodicity at different scales, Physica D 238 (16) (2009) 1668–1679.
[19] D.E. Kirk, Optimal Control Theory: An Introduction, Dover Publications, 2004.
[20] R. Courant, D. Hilbert, Methods of Mathematical Physics, vol. 2, Interscience, New York, 1962.
[21] I.S. Gradshteyn, I.M. Ryzhik, Table of Integrals, Series, and Products, Academic Press, New York, 1980.

Please cite this article in press as: G. Mathew, I. Mezić, Metrics for ergodicity and design of ergodic dynamics for multi-agent systems, Physica D (2010), doi:10.1016/j.physd.2010.10.010